

**1 Negative density dependence promotes persistence of a globally rare yet locally
2 abundant plant species (*Oenothera coloradensis*)**

3 Alice E. Stears^{1*}, Bonnie Heidel², Maria Paniw³, Roberto Salguero-Gómez⁴, Daniel C.

4 Laughlin¹

5 ¹Botany Department and Program in Ecology, University of Wyoming, Laramie, WY;

6 ²Wyoming Natural Diversity Database, University of Wyoming, Laramie, WY;

7 ³Estación Biológica de Doñana, Sevilla, Spain;

8 ⁴Department of Zoology, University of Oxford, Oxford, OX2 6LD, United Kingdom

9 *Corresponding Author: astears@uwyo.edu

10 Acknowledgements: Funding for this project was provided by the Wyoming Native Plant
11 Society Markow Grant, and the U.S. Fish and Wildlife Service (USFWS) through a grant to the
12 Wyoming Natural Diversity Database and the University of Wyoming Botany Department (grant
13 #14AC00827). Collection of seeds for germination experiments was conducted under USFWS
14 Permit #TE085324-2. Data at Soapstone Prairie were collected under permits #1082-2018
15 (2018), #1166-2019 (2019), and #4919647-26 (2020). Data collection at F.E. Warren Air Force
16 Base was conducted with permission and assistance from Alex Schubert, USFWS Fish and
17 Wildlife Biologist.

18 Author Contributions: Alice Stears, Daniel Laughlin, and Bonnie Heidel contributed to study
19 conception and design and collected demographic data. Analysis was performed by Alice Stears
20 with contributions from Daniel Laughlin, Maria Paniw and Roberto Salguero-Gómez. Alice
21 Stears wrote the manuscript with contributions from all authors.

22 Data Availability Statement: All data that has not previously been published will be
23 available from Zenodo. All code will be available to download from a public GitHub repository
24 and archived on Zenodo.

25 **Conflict of Interest Statement:** The authors declare no conflict of interest.

26

Abstract

27 1. Identifying the mechanisms underlying the persistence of rare species has long
28 been a motivating question for ecologists. Classical theory implies that commu-
29 nity dynamics should be driven by common species, and that natural selection
30 should not allow small populations of rare species to persist. Yet, a majority
31 of the species found on Earth are rare. Consequently, several mechanisms have
32 been proposed to explain their persistence, including negative density dependence,
33 demographic compensation, vital rate buffering, asynchronous responses of sub-
34 populations to environmental heterogeneity, and fine-scale source-sink dynamics.
35 Persistence of seeds in a seed bank, which is often ignored in models of population
36 dynamics, can also buffer small populations against collapse.

37 2. We used integral projection models (IPMs) to examine the population dynam-
38 ics of *Oenothera coloradensis*, a rare, monocarpic perennial forb, and determine
39 whether any of five proposed demographic mechanisms for rare species persistence
40 contribute to the long-term viability of two populations. We also evaluated how
41 including a discrete seed bank stage changed population models for this species.

42 3. Including a seed bank stage in population models had a significant positive impact
43 on modeled *O. coloradensis* population growth rate. Using IPMs that included a
44 discrete seedbank state, we found that negative density-dependence was the only
45 supported mechanism for the persistence of this rare species.

46 4. *Synthesis:* IPMs of two populations of the rare species *O. coloradensis* emphasize
47 the importance of including cryptic life stages such as seed banks in demographic

48 models, but fail to provide strong support for most of the proposed mechanisms
49 of rare species persistence. We propose that high micro-site abundance in a
50 spatially heterogeneous environment enables this species to persist, allowing it
51 to sidestep the demographic and genetic challenges of small population size that
52 rare species typically face. These results emphasize that globally rare species can
53 employ many different strategies for persistence, including the somewhat counter-
54 intuitive phenomenon of local abundance. This reinforces the need for customized
55 management and conservation strategies that mirror the diversity of mechanisms
56 that allow rare species persistence.

57 **Introduction**

58 Determining how and why populations of rare species persist has been a goal for ecologists
59 since the discipline's inception (Levins & Culver, 1971; Drury, 1974). Theoretically, low
60 population size is a final step on a trajectory toward extinction (Stanley, 1979) or the first
61 step toward ubiquity (Spear, Walsh, Ricciardi, & Vander Zanden, 2021). Yet, small but
62 stable populations of rare species exist in every ecosystem and taxonomic group (Magurran
63 & Henderson, 2011). In fact, a large proportion of species globally – as many as 35% of
64 plant species, for example— can be considered naturally rare (Enquist et al., 2019). The
65 prevalence of rarity suggests it is an evolutionarily stable strategy rather than a stop along
66 the path toward extinction or invasion, and implies that there must be both fundamental
67 and realized niches that are available for rare species to occupy. A growing body of evidence
68 demonstrates the importance of rare species for biological processes, including their impacts
69 on community stability (Arnoldi, Loreau, & Haegeman, 2019), and functional composition

70 (Burner et al., 2022), which in turn impact ecosystem function (Lyons, Brigham, Traut, &
71 Schwartz, 2005).

72 Effective conservation and management of rare species require an understanding of both
73 the conditions causing rarity initially, and the mechanisms that allow rare species to persist.

74 Causes of rarity can vary from highly-specific habitat requirements (Sgarbi & Melo, 2018), to
75 adverse impacts of anthropogenic environmental change (Vincent, Bornand, Kempel, & Fis-

76 cher, 2020). In order to then persist in a state of rarity, a species must overcome any of mul-
77 tiple potential challenges, primarily the negative effects of demographic, environmental, and
78 genetic stochasticity, defined as random variation in vital rates (e.g., survival, reproduction),

79 abiotic conditions, or genetic allele frequencies (May, 1973). Stochastic deleterious events

80 can cause extirpation or even extinction of rare species, since there may not be enough un-
81 affected individuals or subpopulations to “rescue” the affected population (Nei, Maruyama,

82 & Chakraborty, 1975). Rare species that maintain populations over time typically do so

83 by employing demographic strategies that compensate for the adverse effects of small pop-
84 ulation size. There are five main strategies that allow persistence of rare populations (Fig.

85 1) (Dibner, Peterson, Louthan, & Doak, 2019): negative density-dependence (Rovere &

86 Fox, 2019), demographic compensation (Villellas, Doak, García, & Morris, 2015), vital rate
87 buffering (Pfister, 1998; Hilde et al., 2020), asynchronous responses between subpopulations

88 (Abbott, Doak, & Peterson, 2017), and fine-scale source-sink dynamics (Kauffman, Pollock,

89 & Walton, 2004; Pulliam, 1988). Negative density-dependence occurs when the growth
90 rate (λ) of a population increases at small population size. Demographic compensation oc-

91 curs when different vital rates are affected in opposing ways by the same perturbation in

92 the environment, which can help maintain a relatively constant population λ in response

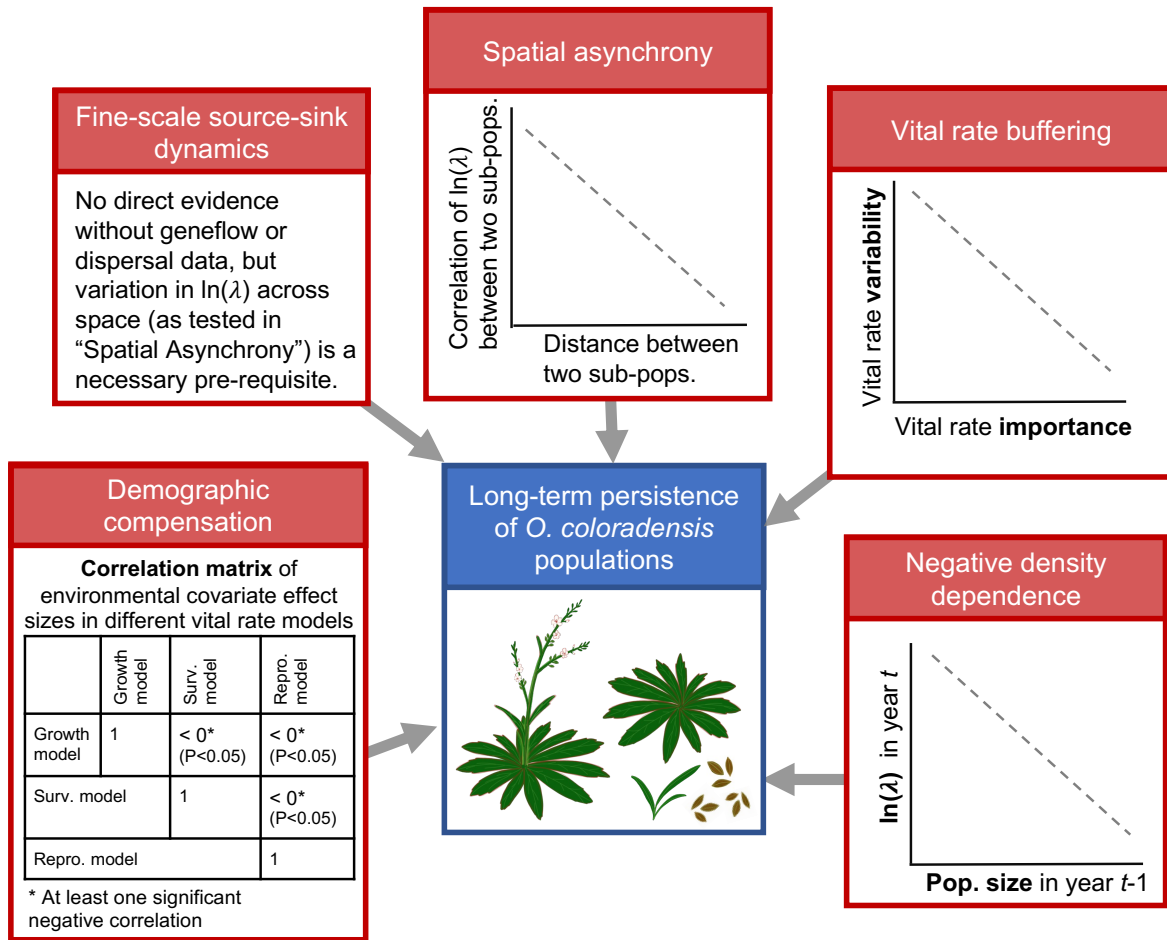
93 to environmental variation. Vital rate buffering occurs when the variability of vital rates
94 decreases as the vital rate becomes more important(i.e., has a higher elasticity), which pre-
95 vents negative effects of temporal variation on the λ across time (Tuljapurkar, 1989). Spatial
96 asynchrony occurs when subpopulations close to one another have different or even opposing
97 growth rates, resulting in a stable population-wide λ . Fine-scale source-sink dynamics occur
98 when there is gene flow between subpopulations that bolsters the size and genetic diversity of
99 very small subpopulations, which again results in a stable population-level λ . Each of these
100 mechanisms can act independently, but also can interact or overlap (Dibner et al., 2019).

101 Here, we identify which of these mechanisms contribute to the persistence or population
102 growth of a rare, endemic plant species, *Oenothera coloradensis* (Rydberg) W.L. Wagner
103 & Hoch (Onagraceae). We use integral projection models (IPMs) (Easterling, Ellner, &
104 Dixon, 2000) that include a discrete seed bank population state. IPMs are flexible models
105 of population dynamics that are constructed using regression models that describe vital
106 rate change across a continuous state variable such as size. IPMs have multiple advantages
107 including better performance with small datasets than traditional matrix models (Ramula,
108 Rees, & Buckley, 2009), and direct incorporation of covariates of interest directly into vital
109 rate models. We built these models with two objectives in mind.

110 Our first objective was to determine if including information about the seed bank signif-
111 icantly altered population models for *O. coloradensis*. Seed banks can serve as important
112 reservoirs of genetic diversity and buffer populations against collapse (Vitalis, Gléménin, &
113 Olivieri, 2004), and can be critical for monocarpic perennials such as *O. coloradensis* that
114 only flower once in their lifetime (Rees et al., 2006). For these reasons, we expected that a
115 soil seed bank is important for *O. coloradensis*, and that its inclusion in IPMs would increase

¹¹⁶ population λ . Seed banks are often not included in population models because their param-
¹¹⁷eters can be very difficult to estimate, but previous work shows that including them can
¹¹⁸significantly alter model outcomes (Paniw, Quintana-Ascencio, Ojeda, & Salguero-Gómez,
¹¹⁹2017; Nguyen, Buckley, Salguero-Gómez, & Wardle, 2019).

¹²⁰ Our second objective was to identify whether any of the five aforementioned persis-
¹²¹tence mechanisms was acting to maintain *O. coloradensis* populations. This species occurs
¹²²in habitats that naturally experience frequent, highly localized disturbance, meaning that
¹²³some subpopulations might be negatively affected by flood, for example, while other nearby
¹²⁴subpopulations are simultaneously thriving due to lack of disturbance. Additionally, pre-
¹²⁵vious matrix population models constructed for this species in the 1990s found substantial
¹²⁶variation in λ across space and time (Floyd & Ranker, 1998). The population-wide pat-
¹²⁷tern of asynchronous habitat disturbance also could make source-sink dynamics important.
¹²⁸ Finally, we have evidence of large fluctuations in the number of plants within subpopula-
¹²⁹tions (Heidel, Tuthill, & Wallace, 2021), which suggest that λ decreases at high population
¹³⁰size and increases at low population size. Therefore, we predicted that density dependence,
¹³¹small-scale source-sink dynamics and asynchronous responses between subpopulations would
¹³²be important mechanisms of persistence for *O. coloradensis*.



¹³³ Figure 1: Evidence that would be required to support each of the five mechanisms that can
¹³⁴ contribute to long-term viability of small populations of rare species.

¹³⁵ Materials and Methods

¹³⁶ Species Description

¹³⁷ *Oenothera coloradensis* (Onagraceae) (Wagner, Krakos, & Hoch, 2013) is an herbaceous,
¹³⁸ monocarpic perennial plant that occurs in frequently disturbed, mesic or wet meadows, and
¹³⁹ riparian floodplains (Fertig, 2000). Non-reproductive individuals consist of a rosette of leaves
¹⁴⁰ with a fleshy taproot. Flowering typically occurs after several years, when individuals bolt

141 and produce a 10-30 cm long floral stalk. Individuals typically die after reproducing–93%
142 of the time in populations we observed. Frequent disturbance such as flooding that re-
143 duces competing species and removes litter is important, especially for successful seedling
144 recruitment (Fertig, 2000). All known *O. coloradensis* populations lie within a 7,000-hectare
145 area that includes southeast Wyoming, northern Colorado, and a small part of southwest
146 Nebraska (Fig. S1). The only known population on Federal land occurs on the F. E. War-
147 ren Air Force Base near Cheyenne, WY (FEWAFB). The Soapstone Prairie Natural Area
148 (Soapstone), owned by the city of Fort Collins, CO, has the largest known population of *O.*
149 *coloradensis* individuals (Heidel et al., 2021). The U.S. Fish and Wildlife Service (USFWS)
150 designated *O. coloradensis* as a “threatened” species under the Endangered Species Act in
151 2000 (Endangered and Threatened Wildlife and Plants, 2000). Managers were concerned
152 that habitat loss due would lead to extinction of this naturally rare species. However, based
153 on subsequent monitoring, the USFWS determined that the species does not appear to be
154 on a trajectory toward extinction, but fluctuates naturally. As a result, *O. coloradensis*
155 was de-listed in 2019. As a result, *O. coloradensis* was de-listed in 2019 (Endangered and
156 Threatened Wildlife and Plants, 2019).

157 Previous work established that *O. coloradensis* λ is particularly impacted by recruitment
158 of seedlings (Floyd & Ranker, 1998). Seed banks are also likely important, since years of
159 high seedling density are not necessarily preceded by years of high rates of flowering and
160 seed production (Heidel et al., 2021). The *O. coloradensis* seed bank has not been studied
161 directly, but a greenhouse seed study showed that an average of 58% of seeds produced by
162 a parent plant are viable, and that a viable seed has a 20% probability of germinating after
163 two months of cold stratification (Burgess, Hild, & Shaw, 2005). These rates did not change

¹⁶⁴ meaningfully over five years (see “Supplementary Material: Species Information” for more
¹⁶⁵ detail).

¹⁶⁶ **Demographic Data Collection**

¹⁶⁷ We conducted a three-year demographic study of *O. coloradensis* across six spatially dis-
¹⁶⁸ tinct subpopulations, three in the FEWAFB population (“Unnamed creek”, “Crow creek”,
¹⁶⁹ and “Diamond creek”) and three at the Soapstone population (“Meadow”, “HQ3” and
¹⁷⁰ “HQ5”)(Table S1; Fig. S1). In early summer 2018, we established three 2x2 m² quadrats
¹⁷¹ in each of these subpopulations, resulting in 18 plots (Table S1). Plants larger than 3 cm
¹⁷² are typically “non-seedling” plants at least one year in age. In each study plot, we tagged
¹⁷³ and mapped each unique “non-seedling” individual and recorded longest leaf length, re-
¹⁷⁴ productive status, and seed production for each (see “Supplementary Information: Seed
¹⁷⁵ Production Estimation” for more detail). Individuals smaller than 3 cm in leaf length are
¹⁷⁶ typically seedlings that germinated that year, occur at high density, and are less likely to
¹⁷⁷ survive than non-seedling plants. Due to these factors, we tallied seedlings in each plot, but
¹⁷⁸ did not map or tag them. In subsequent 2019 and 2020 censuses, we mapped and tagged new
¹⁷⁹ “non-seedling” individuals, and re-measured all surviving individuals from previous years.
¹⁸⁰ Sample size in a given year at a subpopulation ranged from 48 to 1527 individuals (Table
¹⁸¹ S1). All mapping, tagging, and leaf measurements took place between late May and early
¹⁸² July, during the peak of vegetative growth for this species.

183 Environmental Measurements

184 To determine the effect of temporal variation in climate on *O. coloradensis* populations,

185 we used modeled, population-level temperature and precipitation data from PRISM (PRISM

186 Climate Group; Oregon State University, 2021), which we refer to as "environmental covari-

187 ates". We calculated the mean temperature of both the growing season (April in $year_t$ –

188 August in $year_t$) and preceding winter season (September in $year_{t-1}$ – March in $year_t$) for

189 each year of vital rate data collection at FEWAFB and Soapstone. We also calculated total

190 precipitation for each "water year" (October in $year_{t-1}$ to September in $year_t$), which we used

191 in place of growing season precipitation because the shortgrass steppe ecosystem in which *O.*

192 *coloradensis* occurs receives a majority of its annual precipitation in the form of snow, and

193 melting snow from the previous winter likely drives springtime seedling recruitment. Average

194 temperature of the previous winter is also likely important for seedling recruitment, because

195 seed germination is triggered by cold stratification (Burgess et al., 2005). Growing season

196 temperature and precipitation are likely important for growth, survival, and reproductive

197 output of non-seedling plants.

198 Vital Rate Models

199 We used data from the three-year demographic monitoring study detailed above to pa-

200 rameterize models of *O. coloradensis* vital rates (shown in Fig. 2; parameters of fitted vital

201 rate functions are shown in Table S2). We first estimated continuous vital rate functions

202 describing how survival probability, growth, flowering probability, and seed production in

203 $year_{t+1}$ each vary as a function of longest leaf size in $year_t$. We also estimated a continuous

204 vital rate function describing the distribution of new recruit size in $year_{t+1}$. Finally, we es-
205 timated discrete vital rate parameters describing the probability of seeds produced in $year_t$
206 either entering the seed bank or germinating in $year_{t+1}$, as well as the probability of seeds
207 in the seed bank in $year_t$ either staying in the seed bank or germinating in $year_{t+1}$.

208 We first created "global" models for each continuous vital rate (Table. 1). We modeled
209 survival probability ($s(z)$) as a function of log-transformed leaf size ($\ln(size_t)$) using gener-
210 alized linear models with binomial error distributions. Flowering individuals were excluded
211 from the data used to fit survival models, since *O. coloradensis* is a monocarpic perennial
212 that nearly always dies after flowering. We modeled probability of flowering ($Pb(z)$) as a
213 function of using generalized linear models with binomial error distributions, and was pre-
214 dicted by $\ln(size_t)$ plus $\ln(size_t)$ -squared. We modeled seed production ($b(z)$) as a function
215 of $\ln(size_t)$ using negative binomial models because the count data was over-dispersed. We
216 only used data from flowering plants to fit these models, using the "glm.nb" function from
217 the "MASS" R package (Venables & Ripley, 2002). We described growth, or the distribution
218 of plant size in $year_{t+1}$ ($G(z', z)$) as a series of Normal distributions with mean = μ_s and
219 standard deviation = σ_s . μ_s was modeled as a function of $\ln(size_t)$ using a linear model
220 with Gaussian error. σ_s was the residual standard error of this linear model. We described
221 the distribution of recruit size in $year_{t+1}$ ($c_o(z')$) as a Normal distribution with the mean μ_r ,
222 and the standard deviation σ_r . μ_r and σ_r were the mean and standard deviation of observed
223 longest leaf size in $year_{t+1}$.

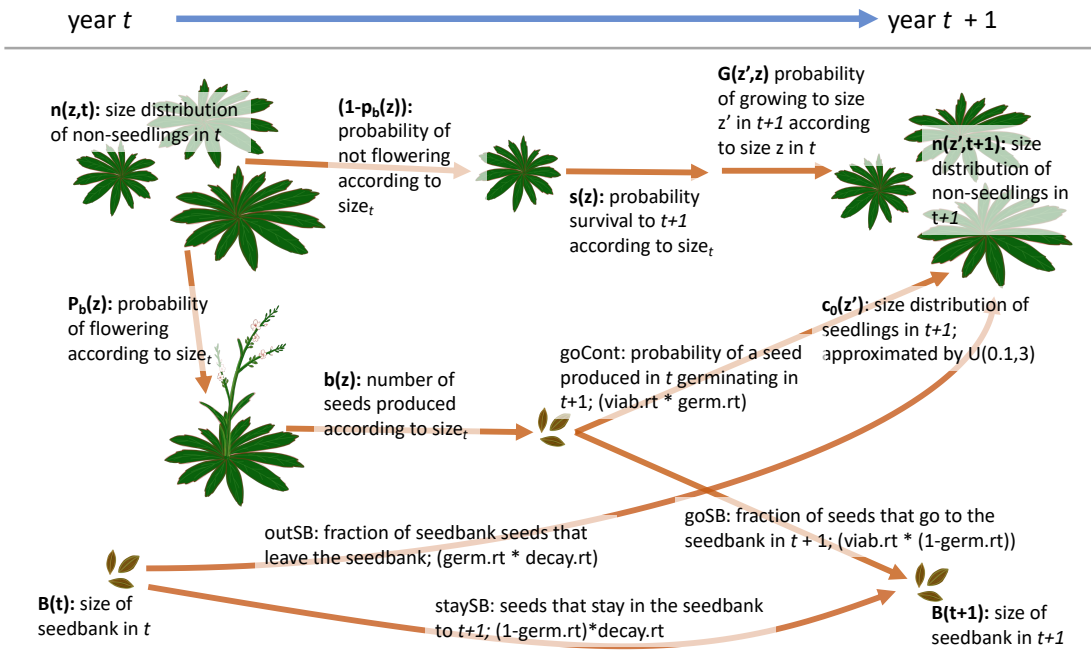
224 We then used these "global" model structures to fit different versions of continuous vital
225 rate functions, each of which described vital rate processes at different temporal and spatial
226 scales. Models were fit using data from the first transition (2018-2019), the second transition

227 (2019-2020), or pooled across both transitions. We also used data from a single subpopula-
228 tion, a single population, or pooled across both populations. We additionally fit models that
229 expanded on the "global" model structures by including density dependence terms and/or en-
230 vironmental covariates (water year precipitation, mean annual growing season temperature,
231 or mean annual winter temperature). When density dependence or environmental covariates
232 were included, we used AIC model selection to confirm that including these covariates im-
233 proved model fit. All continuous vital rate models, regardless of scale, were parameterized
234 using data from "non-seedling plants" as well as seedlings. We incorporated seedlings into
235 the continuous, non-seedling dataset using a process detailed in "Supplementary Information:
236 Seedling Data."

237 We estimated discrete vital rates for seeds uniformly across both populations and years,
238 using data from both greenhouse and field-based germination and seed viability studies.
239 (Table 1). We did not have the data required to determine how these rates changed across
240 subpopulations or in response to abiotic variation, due to the difficulties of estimating *in situ*
241 seed germination and death. We used the following parameters to estimate discrete seed vital
242 rate parameters: viable seed germination rate (germ. rate) = 0.16, viability rate of seeds
243 produced by a parent plant (viab. rate) = 0.58, rate of natural seed death in the seed bank
244 (death rate) = 0.10 (see "Supplementary Information: Discrete Vital Rate Parameters" for
245 more detail).

250 **Population Models**

251 We used estimates of discrete and continuous *O. coloradensis* vital rates to parameterize
252 a suite of integral projection models (IPMs) for *O. coloradensis*. We then used these models



246 Figure 2: Diagram of the *O. coloradensis* life-cycle, labeled with notation used in vital rate
 247 equations shown in Table 1. Based on model structures and notation from: (Paniw et al.,
 248 2017; Merow et al., 2014; Ellner et al., 2016). "germ.rt" = germination rate, "viab.rt" =
 249 viability rate, "decay.rt" = decay rate.

253 to address the objectives outlined in the Introduction.

254 *Objective 1: Importance of the Seed bank Stage:* We used two different IPMs to determine
 255 whether explicitly including a discrete seed bank stage in a population model leads to signif-
 256 icantly different outcomes relative to a model without a seed bank stage. We first created a
 257 density-independent IPM using continuous vital rate functions parameterized with data from
 258 both Soapstone and FEWAFFB. This model had a single continuous, size-based population
 259 state, and did not include a seed bank state (Table 2: IPM "A"; Eqn. 1). This IPM used a
 260 kernel structure where the continuous, above-ground population state ($n(z', t + 1)$) at time

Table 1: Description of vital rates used in *O. coloradensis* IPMs

Vital Rate	Description	Model
$pEstab$	$P(\text{seed produced in } year_t \text{ establishes as a seedling in } year_{t+1})$	$pEstab = \frac{\text{Num. new recruits in } year_{t+1}}{\text{Num. seeds produced in } year_t}$
$goCont$	$P(\text{seed produced in } year_t \text{ germinates in } year_{t+1})$	$goCont = \text{viab. rate} \times \text{germ. rate}$
$outSB$	$P(\text{seed bank seed in } year_t \text{ germinates in } year_{t+1})$	$outSB = \text{germ. rate} \times (1 - \text{death rate})$
$goSB$	$P(\text{seed produced in } year_t \text{ goes into the seed bank in } year_{t+1})$	$goSB = \text{viab. rate} \times (1 - \text{germ. rate})$
$staySB$	$P(\text{seed bank seed in } year_t \text{ stays in the seed bank in } year_{t+1})$	$staySB = (1 - \text{germ. rate}) \times (1 - \text{death rate})$
$Survival(s(z))$	$P(\text{survival from } year_t \text{ to } year_{t+1})$	$\text{logit}(\text{survival}) \sim \beta_0 + \beta_1(\ln(\text{size}_t)) + \epsilon$
$Flowering(Pb(z))$	$P(\text{flowering in } year_t)$	$\text{logit}(\text{flowering}) \sim \beta_0 + \beta_1(\ln(\text{size}_t)) + \beta_2(\ln(\text{size}_t)^2) + \epsilon$
$Seed\ prod.(b(z))$	$\text{Seed production in } year_t$	$\exp(\text{seed number}) \sim \beta_0 + \beta_1(\ln(\text{size}_t)) + \epsilon$
$Growth(G(z', z))$	$\text{Distribution of } \ln(\text{longest leaf size}) \text{ in } year_t$	$G(z', z) = N(\mu_s, \sigma_s);$ $\mu_s \sim \beta_0 + \beta_1(\ln(\text{size}_t)) + \epsilon;$ $\sigma_s \sim RSE(\beta_0 + \beta_1(\ln(\text{size}_t)) + \epsilon)$
$Recruit\ size(c_o(z'))$	$\text{Distribution of new recruit size in } year_t$	$c_o(z') = N(\mu_r, \sigma_r);$ $\mu_r = \text{mean}(\text{size of recruits in } t);$ $\sigma_r = \text{stnd. dev. (size of recruits in } t)$

* RSE = residual standard error

261 $t + 1$ was described by the following equation:

$$n(z', t + 1) = \int_L^U (1 - P_b(z)) s(z) G(z', z) n(z, t) dz + pEstab \int_L^U P_b(z) b(z) c_o(z') n(z, t) dz \quad (1)$$

262 We then created an IPM that included both a continuous, size-based stage for above-

263 ground individuals, and a discrete seed bank state (Table 2: IPM “B”; Eqns. 2 & 3) (Ellner

264 & Rees, 2006; Rees et al., 2006; Paniw et al., 2017). This model used the same continuous

265 vital rate functions as IPM A, but also included discrete values describing the probabilities

266 of seeds produced in $year_t$ germinating or going into the seeds bank in $year_{t+1}$, and the

267 probabilities of seeds in the seed bank in $year_t$ germinating or persisting in the seed bank in

268 $year_{t+1}$. This IPM with two population states used a kernel structure where the continuous,

269 above-ground population state ($n(z', t + 1)$) and the seed bank state ($B(t + 1)$) at time $t + 1$

270 were described by the following equations:

$$n(z', t + 1) = \int_L^U (1 - P_b(z)) s(z) G(z', z) n(z, t) dz + \\ goCont \int_L^U P_b(z) b(z) c_o(z') n(z, t) dz + outSB \quad (2)$$

$$B(t + 1) = goSB \int_L^U P_b(z) b(z) n(z, t) dz + B(t) staySB \quad (3)$$

Table 2: A description of the data used to create each IPM, as well as the covariates included in the vital rate models used in that IPM. $\ln(\lambda)$ estimates and 95% bootstrap confidence intervals of $\ln(\lambda)$ are also shown for each IPM.

IPM	Data Included		Transition	Covariates	$\ln(\lambda)$ (95% CI)
	Each pop.	Each subpop.			

		Continuous state only	Continuous + seed bank state	All subpopulations	Soapstone FEWAFB	Unnamed Creek Diamond Creek Crow Creek Meadow HQ3 HQ5	All Transitions	2018-2019 2019-2020	Density dependence	Environmental covariates	
A	x		x				x			0.27 (0.269, 0.271)	
B		x	x				x			0.65 (0.648, 0.650)	
C	x			x			x			0.48 (0.477, 0.489)	
D	x				x		x			1.13 (1.124, 1.142)	
E	x					x	x			0.74 (0.725, 0.746)	
F	x					x	x			0.54 (0.520, 0.551)	
G	x					x	x			0.395 (0.378, 0.401)	
H	x						x	x		0.53 (0.526, 0.540)	
I	x			x			x		x	0.59 (0.576, 0.637)	
J	x				x		x		x	0.63 (0.611, 0.723)	
K	x				x		x		x	-0.10 (-0.135, 0.063)	
L	x					x	x		x	-0.20 (-0.229, -0.167)	
M	x					x	x		x	1.31 (1.294, 1.354)	
N	x						x	x	x	2.31 (2.297, 2.33)	
S	x			x			x		x	x	0.58
T	x				x		x		x	x	0.51
U	x				x		x		x	x	0.90

V	x			x	x	x	x	-0.27
W	x			x	x	x	x	-0.18
X	x			x	x	x	x	0.76
AA	x	x		x				0.50 (0.497, 0.501)
BB	x		x		x			0.73 (0.729, 0.733)
CC	x			x		x		0.38 (0.370, 0.388)
DD	x			x		x		1.56 (1.545, 1.572)
EE	x			x		x		0.90 (0.864, 0.904)
FF	x			x		x		0.62 (0.592, 0.637)
GG	x			x		x		0.73 (0.727, 0.753)
HH	x			x		x		1.11 (1.108, 1.126)
II	x		x			x		0.50 (0.492, 0.513)
JJ	x			x		x		0.71 (0.692, 0.726)
KK	x			x		x		0.76 (0.739, 0.774)
LL	x			x		x		0.41 (0.378, 0.448)
MM	x			x		x		0.03 (0.013, 0.040)
NN	x			x		x		-0.10 (-0.112, -0.097)

*Note: We did not calculate bootstrap 95% confidence intervals for $\ln(\lambda)$ of models "S" –"X", since only vital rate parameters and not lambda values from these models were used in further analysis.

271 In equations for both types of IPMs, z is the distribution of plant longest leaf size (measured
 272 as longest leaf length) in the current year ("size_t"), z' is the distribution of plant longest leaf size
 273 in the next year ("size_{t+1}"), and U and L are the upper and lower limits of leaf size. $G(z', z)$
 274 is the vital rate function describing size_{t+1} as a function of size_t. The vital rate functions $s(z)$,

275 $Pb(z)$, and $b(z)$ describe the relationship between $size_t$ and survival probability of non-flowering
276 plants, flowering probability, and seed production of flowering plants, respectively. $c_o(z')$ is the
277 distribution of aboveground recruit $size_{t+1}$. $goCont$, $outSB$, $goSB$, and $staySB$ are discrete
278 parameters that determine seed bank dynamics. $goCont$ is the probability that a seed produced in
279 year t germinates as a seedling in year $t + 1$, $outSB$ is the probability that a seed from the seed
280 bank in year t germinates as a seedling in year $t + 1$, $goSB$ is the probability that a seed produced
281 in year t goes into the seed bank in year $t + 1$, and $staySB$ is the probability of a seed from the
282 seed bank in year t persisting in the seed bank in year $t + 1$ (Paniw et al., 2017) (Table 1). $pEstab$
283 is the probability that a seed produced in year t establishes as a seedling in year $t + 1$.

284 We used these vital rate functions and discrete parameters to construct discretized IPM kernels,
285 which were numerically implemented using the “midpoint rule” method (Easterling et al., 2000)
286 with 500 bins, an upper size limit corresponding to 120% of the maximum observed longest leaf
287 size and a lower size limit corresponding to 80% of the minimum simulated seedling size of 0.1 cm.
288 We then used eigen analysis of these kernels to estimate the log-transformed asymptotic population
289 growth rate ($\ln(\lambda)$), damping ratio, stable size distribution, and reproductive value (Caswell, 2001;
290 Ellner, Childs, & Rees, 2016). We used 1000 iterations of bootstrap resampling to estimate 95%
291 bootstrap confidence intervals (95% CIs) for each continuous vital rate parameter included in each
292 IPM, as well as each estimate of $\ln(\lambda)$ (Merow et al., 2014; Fieberg, Vitense, & Johnson, 2020).
293 We were unable to estimate CIs for discrete seed bank parameters because they were drawn from
294 a previous publication. We used perturbation analysis to determine the sensitivity and elasticity
295 of $\ln(\lambda)$ to changes in germination rate, viability rate, seed survival rate and each continuous vital
296 rate model (Morris & Doak, 2002). Finally, to determine whether including a discrete seed bank
297 state significantly altered our population model, we compared the asymptotic $\ln(\lambda)$ and associated
298 95% CI between IPM "A" and IPM "B."

299 Objective 2: Evaluating Persistence Mechanisms

300 To evaluate whether any of the demographic mechanisms of rare species persistence outlined in

301 Fig. 1 act in populations of *O. coloradensis*, we fit a series of IPMs that each used different subsets

302 of data as well as additional covariates in vital rate functions to account for density dependence and

303 environmental variation (Table 2: IPMs “C” – “NN”). These IPMs all had a mathematical form

304 equivalent to that of IPM “B” described above, with a discrete seed bank state, and a continuous,

305 size-based stage for above-ground individuals (Eqns. 2 & 3). We then used each of these IPMs, as

306 well as the vital rate functions used to construct them, to evaluate a different persistence mechanism.

307 Details of this process for each persistence mechanism are provided below.

308 *Negative Density Dependence:* In order to determine the importance of density dependence in

309 *O. coloradensis* subpopulations, we used IPMs and vital rate functions that were fit uniquely for

310 each subpopulation using data from both transitions. However, one set of IPMs included population

311 size in the current year in vital rate models, while another set of IPMs did not (density-independent

312 IPMs: “C”–“H” in Table 2; density-dependent IPMs: “I”-“N”). We used AIC to identify significant

313 differences between vital rate models with and without density dependence terms. We also used

314 results from subpopulation-level IPMs (Table 2: IPMs ”CC”-”NN”) for each transition to identify

315 relationships between subpopulation size in $year_t$ and $\ln(\lambda)$ (as in Fig. 1), as well as subpopulation

316 size in $year_t$ and the ratio of population size in $year_{t+1}$ and subpopulation size in $year_t$. In

317 addition to population size information and $\ln(\lambda)$ values from our IPMs, we also used population

318 sizes and $\ln(\lambda)$ values from a previously-published demographic study of *O. coloradensis* at the three

319 FEWAFB subpopulations that we also monitored (Floyd & Ranker, 1998). A negative relationship

320 between population size in $year_t$ and either $\ln(\lambda)$ or the ratio of population size in year $t + 1$ to

321 population size in $year_t$ would provide evidence for negative density dependence. Additionally,

322 significant differences between models with and without population size predictor terms would
323 constitute evidence for density dependence.

324 *Demographic Compensation:* To test for demographic compensation, we calculated the correlation
325 between environmental covariate coefficients in different vital rate models. We used vital rate
326 models that were fit using data from each subpopulation and both transitions, and that included
327 covariates for density dependence and as well as environmental covariates that improved model
328 fit (vital rate models from IPMs “S”-“X” in Table 2). We tested the significance of negative cor-
329 relations between environmental covariate coefficients using a randomization procedure similar to
330 that used by Villegas et al. (2015), where we randomly assigned an environmental covariate coeffi-
331 cient drawn from the observed distribution of values for that coefficient to each vital rate function,
332 calculated a correlation matrix between those coefficients in each vital rate function, and counted
333 the number of negative correlations in that matrix. We repeated this procedure 10,000 times to
334 generate a null distribution of the expected number of negative correlations between environmental
335 coefficients. We compared the observed number of negative correlations to these expected distri-
336 butions to determine statistical significance. We could not test for demographic compensation in
337 discrete seed bank vital rate parameters because we did not know how they varied according to
338 environmental conditions. A negative correlation between coefficients for the same covariate in dif-
339 ferent vital rate models would indicate that demographic compensation was taking place (Villegas
340 et al., 2015; Dibner et al., 2019)(Fig. 1). For example, if soil moisture had a positive effect on
341 growth but a negative effect on survival, this would be evidence for demographic compensation.

342 *Vital Rate Buffering:* We tested for the presence of vital rate buffering in *O. coloradensis* pop-
343 ulations by comparing the variability of vital rates to their importance. We used an approach that
344 scales both the standard deviation (variability metric) and sensitivity (importance metric) of vital
345 rates, allowing for a fair comparison of variability and importance across vital rates with fundamen-

346 tally different relationships between their mean and variance (McDonald et al., 2017). Vital rates
347 that are probabilities are constrained between zero and one and thus typically have small variance
348 as the mean approaches these limits, while other vital rates are only constrained by zero and thus
349 typically have variances that increase as the mean increases (Gaillard & Yoccoz, 2003). To enable
350 a fair comparison between these different categories of vital rates, we calculated their importance
351 and variability metrics in different ways. Importance of probability vital rates corresponded to the
352 logit variance stabilized sensitivity, and variability corresponded to the standard deviation of the
353 logit transformed vital rate values. Importance of non-probability vital rates corresponded to the
354 log-scaled sensitivity (or elasticity), and variability was corresponded to standard deviation of the
355 log-transformed vital rate values (McDonald et al., 2017; Morris & Doak, 2002; Link, William A,
356 Paul F Doherty, Fr., 2002).

357 We used IPM “B” to calculate elasticity or logit VSS values for each discrete and continuous
358 vital rate. We calculated the scaled standard deviation for each continuous vital rate function using
359 the vital rates that were fit uniquely for each subpopulation and each transition (Table 2: IPMs
360 “CC” - “NN”). Because we did not have site-level information about discrete seed bank vital rates,
361 we simulated both the maximum and minimum possible standard deviations for each discrete vital
362 rate. We then proceeded with two comparisons of vital rate variability and importance, one using
363 the maximum possible discrete vital rate standard deviation, and another using the minimum. In
364 order to determine the correlation between a single importance/variability value pair for discrete
365 vital rates and a string of value pairs for continuous vital rate functions, we calculated mean
366 importance and variability values for each continuous vital rate function. A significant negative
367 correlation between the mean or absolute scaled importance (logit VSS or elasticity) and mean or
368 absolute variability (standard deviation of logit or log-transformed vital rates) across all vital rates
369 would constitute support for the presence of vital rate buffering in this species (Fig. 1).

370 *Asynchronous Responses and Source-Sink Dynamics:* To determine whether *O. coloradensis*

371 subpopulations showed asynchronous responses to environmental variation, we made a correlation

372 matrix to determine how change in $\ln(\lambda)$ from year to year was correlated across each subpopulation,

373 using values of $\ln(\lambda)$ derived from IPMs for each subpopulation (Table 2: IPMs “C”-“H”). We used

374 the “mantel()” function from the “vegan” R package to perform a Mantel test, which determined if

375 the Spearman correlation of $\ln(\lambda)$ across subpopulations was significantly related to the Euclidean

376 distance between each subpopulation (Oksanen et al., 2020). A negative relationship between the

377 distance between subpopulations and degree of correlation of $\ln(\lambda)$ would constitute evidence for

378 spatial asynchrony between subpopulations (Fig. 1).

379 Because we did not have information about gene flow between subpopulations of *O. coloradensis*

380 via pollination or seed dispersal, it was impossible to directly measure whether fine-scale source-

381 sink dynamics were acting in these populations. However, because variation in $\ln(\lambda)$ across space

382 is a prerequisite for source-sink dynamics, the tests for spatial asynchrony in subpopulations can

383 also provide evidence for the existence of source-sink dynamics. Again, this would be a negative

384 relationship of distance between subpopulations and correlation of subpopulation $\ln(\lambda)$ (Fig. 1).

385 Results

386 Vital Rate Models

387 Larger non-reproductive plants were more likely to survive than smaller plants (Fig. 3A).

388 Plants below ~ 7.5 cm were likely to be larger, while plants larger than ~ 7.5 cm were likely to be

389 smaller the following year (Fig. 3 B). Flowering probability was best approximated as a quadratic

390 polynomial, where flowering probability peaked at 12 cm leaf length, and plants with the largest

391 leaves exhibited low flowering probability (Fig. 3 C). The number of seeds that a reproductive

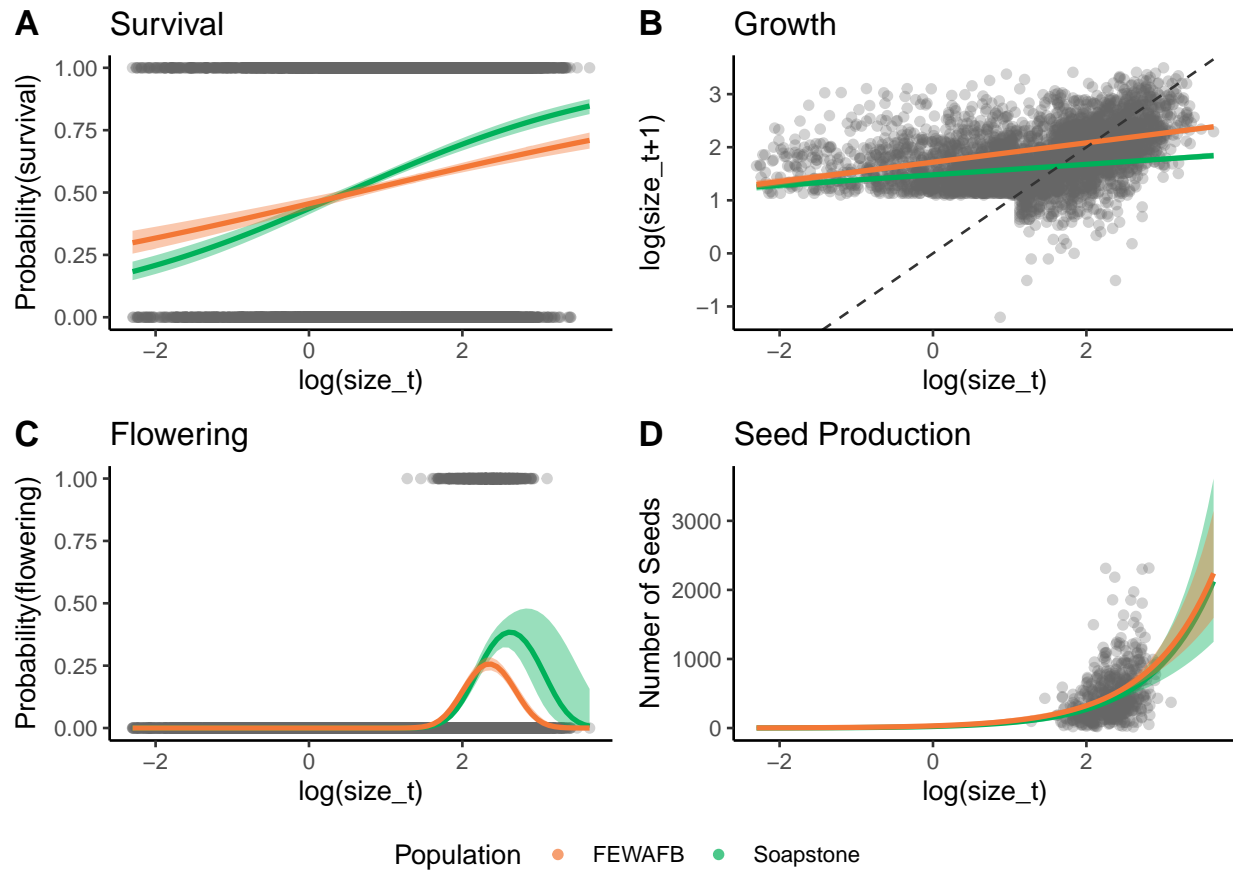
392 plant produced increased sharply with leaf size (Fig. 3 D). The inclusion of additional covariates
393 did not alter the overall shape or sign of the relationships between leaf size and vital rates, so
394 models shown in Figure 3 did not include any additional covariates beyond leaf size.

395 **Objective 1: Importance of the Seed bank Stage**

396 *Integral Projection Models:* We found that including a discrete seed bank stage in IPMs for *O.*
397 *coloradensis* significantly increased $\ln(\lambda)$. The continuous state-only IPM (Table 2: IPM “A”) pre-
398 dicted an asymptotic $\ln(\lambda)$ of 0.27 for all populations (95% CI: 0.269 - 0.271), while the continuous
399 + discrete state IPM (Table 2: IPM “B”) predicted an asymptotic $\ln(\lambda)$ of 0.65 (populations (95%
400 CI: 0.648 - 0.650). All subsequent IPM results refer to models that included a discrete seed bank
401 state.

402 The simplest two-state IPMs that excluded density dependence and environmental variation
403 indicated that both the Soapstone and FEWAFB populations had positive $\ln(\lambda)$ values (Table 2:
404 Soapstone - IPM “AA”, $\ln(\lambda) = 0.50$; FEWAFB – IPM “BB”, $\ln(\lambda) = 0.73$). The Diamond Creek
405 subpopulation at FEWAFB had the highest $\ln(\lambda)$ from 2018 to 2020 (Table 2: IPM “D”, $\ln(\lambda) =$
406 1.13), while the HQ3 subpopulation at Soapstone had the lowest growth rate (Table 2: IPM “G”,
407 $\ln(\lambda) = 0.395$). Almost all additional IPMs identified a positive $\ln(\lambda)$ (Table 2).

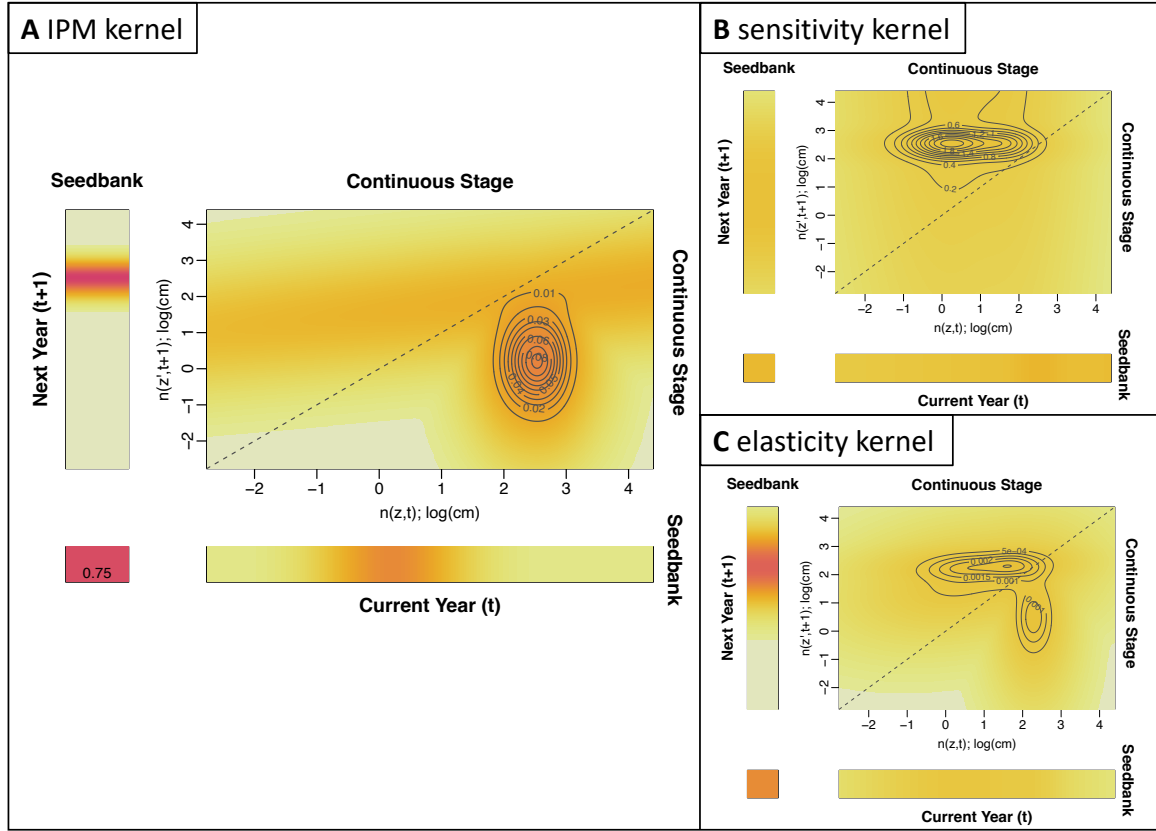
415 A density-independent, discretized IPM kernel (made using IPM “B” in Table 2) calculated
416 transition probabilities within and between the discrete and continuous stages of the *O. coloradensis*
417 life cycle when all populations and transitions were considered together (Fig. 4 A). Relative to other
418 demographic transitions, there was a high probability that seeds stayed in the seed bank, and a
419 high probability that seeds from medium-sized adult plants go into the seed bank in the next year.
420 Population λ was most sensitive to the rates at which seeds were produced by adult plants and
421 stayed in the seed bank (Fig. 4 C).



408 Figure 3: The effect of current year leaf size ($\ln(\text{size}_t)$) on vital rates in monitored *O.*
 409 *coloradensis* populations. Data for all sites and all transitions are shown. Lines indicate
 410 vital rate functions for each population, fit using the "global" model structure described in
 411 the Methods section. Bands around each line show 95% confidence intervals. The dashed
 412 line in panel **B** shows a 1:1 line. The sharp cut-off in $\ln(\text{size}_{t+1})$ in panel **B** is due to the
 413 fact that two-year-old plants could not be seedlings, which were classified as any plant less
 414 than 3 cm in size.

428 Objective 2: Evaluating Persistence Mechanisms

429 *Negative Density Dependence:* We found evidence that negative density-dependence occurred
 430 in subpopulations of *O. coloradensis*. AIC comparison of continuous vital rate models indicated
 431 that density-dependent models were better predictors of the majority of vital rates than density-
 432 independent models in most subpopulations (Table 3). Models that included population size in
 433 the previous year as a covariate were better predictors of growth in five of six subpopulations.



422 Figure 4: Visualizations of the *O. coloradensis* IPM kernels. **(A)** The IPM kernel for *O.*
 423 *coloradensis*. This kernel shows a density-independent IPM constructed using all data from
 424 all transitions (IPM "B"). **(B)** Sensitivity of the IPM kernel. **(C)** Elasticity of the IPM
 425 kernel. In all panels, color indicates probability, with darker colors corresponding to higher
 426 probability, and lighter colors corresponding to lower probability. The dashed line shows a
 427 1:1 line.

434 Density dependent models were better predictors of survival and seed production in four out of
 435 six subpopulations, and density dependent models of flowering were better in one subpopulation.
 436 Recruit size distribution was not affected by density dependence. The vital rate models for the
 437 Meadow population at Soapstone were least affected by density dependence. Although density
 438 dependence was important for *O. coloradensis* in many situations, it appeared only to be acting to
 439 decrease λ at high density (as in the highly dense Diamond Creek or HQ5 subpopulations), but not
 440 clearly increasing lambda at low density (as in the sparsely populated Meadow subpopulation). We

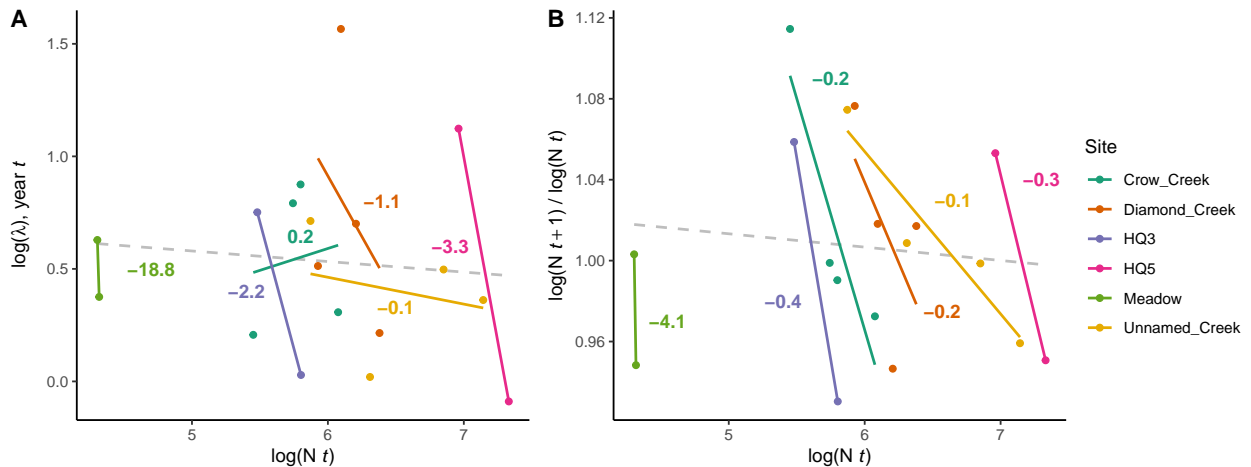
441 also found that, within a subpopulation, $\ln(\lambda)$ was generally higher when subpopulation size was
442 smaller (Fig. 5 A). Similarly, there was a negative relationship within each subpopulation between
443 subpopulation size in $year_t$ and the ratio of subpopulation size in $year_{t+1}$ to subpopulation size in
444 $year_t$ (Fig. 5 B and D); Interestingly, these negative relationships are generally pronounced at the
445 subpopulation level, but are weak when examining data across all subpopulations.

446 *Demographic Compensation:* We did not find evidence of demographic compensation in *O. col-*
447 *oradensis* populations. While there were negative correlations between the effect of mean growing
448 season temperature on vital rates for five combinations of vital rates, none of these correlations
449 were significant (Table 4). The only significant correlation, between temperature coefficients in
450 growth and survival models, was positive. Ten thousand correlations of randomly assigned coef-
451 ficients found that the number of negative correlations in a matrix can be described by a normal
452 distribution with a mean of 4.97 and a standard deviation of 1.60. Using this distribution as a null
453 model, there was a 50.7% probability of observing five negative correlations. Although there is no
454 significant evidence for demographic compensation, it is notable that the effect of mean growing
455 season temperature on distribution of recruit size was negatively correlated with the effect of grow-
456 ing season temperature on all other vital rates. We were only able to compare coefficients across
457 vital rate models for mean growing season temperature, because including precipitation and mean
458 winter temperature as covariates resulted in overfitting in some cases.

475 *Vital Rate Buffering:* We did not find evidence of vital rate buffering in the *O. coloradensis*
476 populations we observed. Vital rate importance (either logistic VSS or elasticity) and variability
477 (corrected SD) were not significantly negatively correlated, regardless of the simulated standard
478 deviation for discrete vital rates we used (Fig. 6; correlation with minimum discrete vital rate SD
479 (**A**): $r = 0.43$, $P = 0.25$; correlation with maximum discrete vital rate SD (**B**): $r = -0.07$, $P =$
480 0.85). As a vital rate became more important for determining $\ln(\lambda)$, it did not become significantly

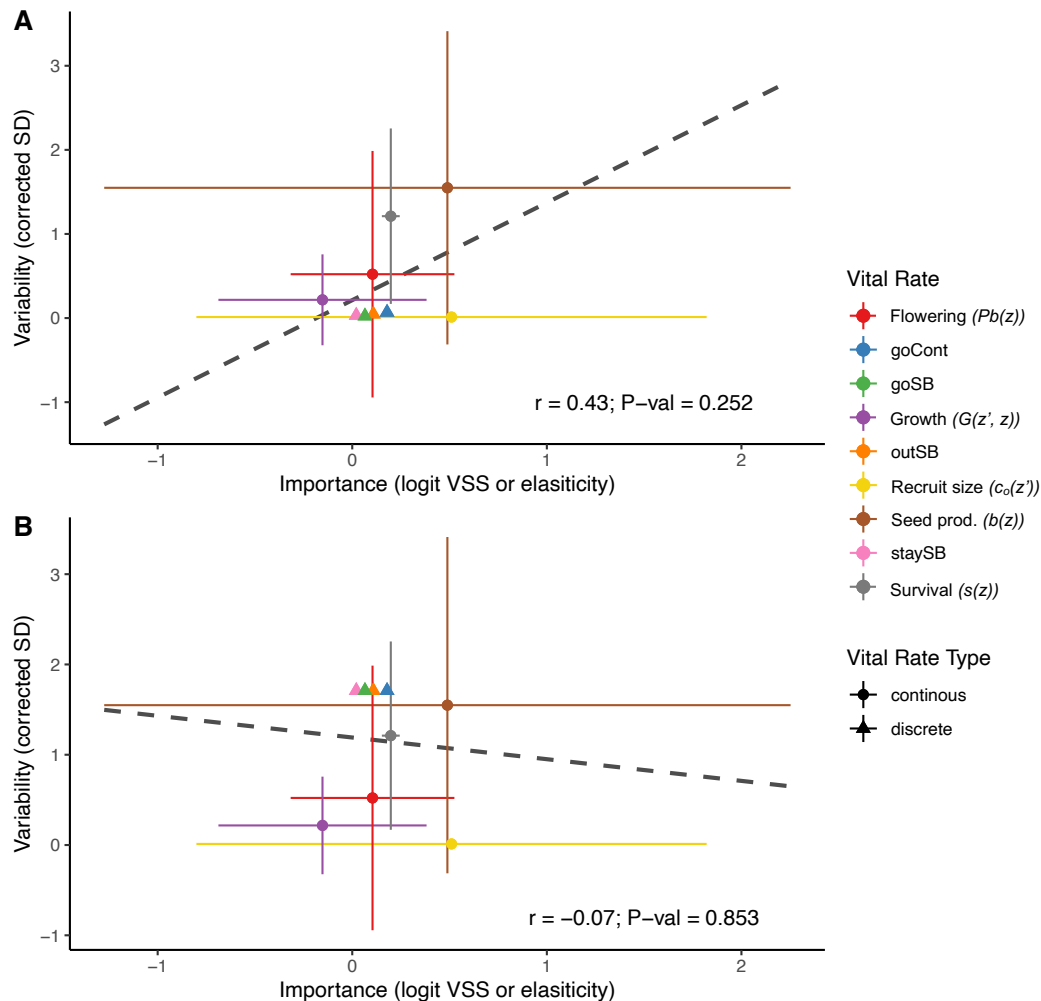
459 Table 3: Comparison of vital rate models with and without density dependence. Values
 460 show the ΔAIC , or difference between the AIC of density independent (DI) and density
 461 dependent (DD) models. Bold text indicates that the $|\Delta\text{AIC}|$ value is > 3 , which means
 462 that including a term for density dependence substantially changed that vital rate model.
 463 A positive $|\Delta\text{AIC}|$ indicates that including density dependence improved the model, while
 464 a negative value indicates that including density dependence made model fit worse. AIC
 465 values for DI and DD values can be found in Table S3.

Vital Rate Model	Subpopulation Data					
	Crow Creek	Diamond Creek	Unnamed Creek	HQ5	HQ3	Meadow
Survival	18.74	107.28	-0.41	320.33	78.82	-0.70
Growth	3.73	22.15	30.811	458.15	30.45	2.66
Flowering	-1.63	-0.44	0.45	54.52	-1.76	-1.72
Seed production	6.41	14.02	-1.29	3.71	4.12	-1.35
Recruit size	-1.93	1.61	-1.93	-1.97	-1.23	-1.99



466 Figure 5: (A) Within the same subpopulation, $\ln(\lambda)$ calculated from IPMs decreases as
 467 population size increases. (B) Within each subpopulation, $\ln(\lambda)$ calculated by change in
 468 population size from $year_t$ to $year_{t+1}$ also decreases as population size increases. In A and B,
 469 each point represents values calculated from data from one transition in one subpopulation.
 470 Solid lines show linear regressions of the relationships between $\ln(N_t)$ and the respective
 471 response variable in each subpopulation. Numbers adjacent to these solid lines show the
 472 slope of each relationship, and are color-coded by subpopulation. Dashed grey lines show
 473 linear regressions of the relationships between $\ln(N_t)$ and the respective response variable
 474 across all subpopulations.

481 less variable, as it would if vital rate buffering was occurring (Fig. 1).



482 Figure 6: The relationship between variability of each vital rate (measured by corrected
 483 standard deviation) and its importance (measured by logit VSS or elasticity) does not show
 484 support for vital rate buffering. **(A)** With the minimum possible simulated discrete vital rate
 485 variability, there is a positive but insignificant correlation between vital rate variability and
 486 importance ($r = 0.43, P = 0.25$). **(B)** Using the maximum possible simulated discrete vital
 487 rate variability, there is a negative but insignificant correlation between vital rate variability
 488 and importance ($r = -0.07, P = 0.85$). Triangles indicate importance and variability for
 489 discrete vital rate parameters, while circles indicates the means of importance and variability
 490 across an entire continuous vital rate function. Error bars around continuous vital rate means
 491 span the the 5th to 95th percentiles of either importance or variability values calculated for
 492 an entire continuous vital rate function. Dashed lines show the correlation between (mean)
 493 variability and (mean) importance across all vital rates.

494 *Asynchronous Responses and Source-Sink Dynamics:* We did not find evidence of asynchronous

responses to environmental variation in *O. coloradensis* populations. There was not a significant relationship between the Spearman correlation of $\ln(\lambda)$ between subpopulations and their spatial proximity (Mantel statistic = 0.396, $P = 0.06$). We also performed Mantel tests using $\ln(\lambda)$ correlation and distance matrices calculated uniquely for each population, and did not find evidence for asynchronous responses (Soapstone: Mantel statistic = -0.659, $P = 0.83$; FEWAFB: Mantel statistic = 0.798, $P = 0.33$). We did, however, find a positive relationship between correlation of $\ln(\lambda)$ and distance between subpopulations at Soapstone, and a negative relationship between subpopulations at FEWAFB. Collectively, these results fail to provide support for both asynchronous responses and fine-scale source-sink dynamics in these *O. coloradensis* populations.

Table 4: Pearson correlations between mean growing season temperature coefficients in each continuous vital rate function. Below each correlation value is the P value for that correlation. Bold text indicates a significant correlation.

		Vital Rate				
		<i>Flowering</i>	<i>Survival</i>	<i>Growth</i>	<i>Seed</i>	<i>Recruit</i>
					<i>Prod.</i>	<i>Size</i>
Vital Rate	<i>Flowering</i>	1.00 (0)	0.474 (0.342)	0.136 (0.797)	-0.073 (0.890)	-0.786 (0.064)
	<i>Survival</i>		1.00 (0)	0.886 (0.019)	0.675 (0.141)	-0.3570 (0.237)
			<i>Growth</i>	1.00 (0)	0.664 (0.150)	-0.270 (0.606)
				<i>Seed Prod.</i>	1.00 (0)	-0.432 (0.393)
					<i>Recruit Size</i>	1.00 (0)

507 **Discussion**

508 Our demographic analysis of the two largest known populations of the globally rare *Oenothera*
509 *coloradensis* evaluated the importance of seed banks to population dynamics and the demographic
510 mechanisms that allow this rare species to persist. We found that including information about
511 cryptic life stages alters the outcomes of the population model (Paniw et al., 2017; Nguyen et
512 al., 2019), and that *O. coloradensis* populations show signs of negative density-dependence at the
513 subpopulation scale (Fig. 5; Table 3). However, these populations do not show substantial evidence
514 of demographic compensation, vital rate buffering, spatial asynchrony, or fine-scale source-sink
515 dynamics. This may indicate that while these mechanisms may be important for the persistence of
516 many small populations of rare plants, they are not strictly necessary in all cases.

517 Including a discrete seed bank state in an IPM increased the asymptotic population growth
518 rate ($\ln(\lambda)$) compared to an IPM with only a continuous, size-based state, although both growth
519 rates were still positive (Table 2: with seed bank: IPM “B”, $\ln(\lambda) = 0.65$; without seed bank:
520 IPM “A”, $\ln(\lambda) = 0.27$). The importance of including the seed bank in the model was consistent
521 with our expectations, and also aligns with the conventional notion that seed banks can act as
522 buffers against stochastic causes of population decline. The discrete rates for the probability of
523 persisting and transitioning out of the seed bank have high elasticity in the IPMs in which they
524 are included, but not the highest elasticity of any vital rate (Fig. 4 C). The rate at which seeds
525 produced by adult plants in $year_t$ go into the seed bank in $year_{t+1}$ is the vital rate function with
526 highest elasticity. Previous matrix population models of *O. coloradensis* without a seed bank state
527 that were constructed in the 1990s identified the emergence rate of new seedlings as the vital rate
528 most important for determining $\ln(\lambda)$ (Floyd & Ranker, 1998). Our finding that seed bank state
529 transitions are important for this species aligns with this previous result, since rate of seedling

530 emergence is the above-ground plant vital rate that is closest to the seed bank in this plant's life
531 cycle. An important caveat to our comparison of models with and without seed bank stages is
532 the fact that the seed bank vital rate parameters we used were inferred from laboratory tests of
533 germination and viability rates, which may be imperfect representations of *in-situ* rates of viability
534 and germination. The annual rate of seed death (10%) was inferred from an *in-situ* study, but
535 is likely imprecise because of low sample size. Regardless of these potential sources of error, our
536 results reinforce the fact that the seed bank can be an important element of a perennial plant's life
537 cycle, and if possible, should be modeled explicitly based on *in-situ* estimates of the probability of
538 seeds going into, persisting in, and emerging from the seed bank.

539 We found evidence that, of the five proposed demographic mechanisms of small population per-
540 sistence, negative density dependence was the only one acting in these *O. coloradensis* populations.
541 Including population size in the previous year as a covariate in vital rate models typically improved
542 model fit, suggesting that density dependence is an important driver of growth, survival, and repro-
543 duction (Table 3). Within a single subpopulation, $\ln(\lambda)$ and the ratio of population size in $year_{t+1}$
544 to $year_t$ was generally higher when population size in $year_t$ was smaller (Fig. 5), which indicates
545 that negative density dependence prevents subpopulations from crashing when their population
546 size is very small. However, this pattern of higher growth rate at low population sizes did not exist
547 when considering all subpopulations together (Fig. 5). This could indicate that each subpopulation
548 is close to its carrying capacity for *O. coloradensis*. This may indicate that the number of indi-
549 viduals is close to carrying capacity in each subpopulation, and that growth rate increases when
550 the population size in a given subpopulation is small in comparison to its subpopulation-specific
551 carrying capacity. *O. coloradensis* vital rates had correlated responses to variation in the abiotic
552 environment (Table 4), which is the inverse of what is expected if demographic buffering is taking
553 place. It is possible that a signal of demographic buffering would appear if we considered different

554 abiotic variables such as disturbance frequency, or had more data. Vital rate buffering also was not
555 identified, either with the minimum or maximum possible simulated discrete vital rate variability
556 (Fig. 6). Vital rates with higher variability (higher SD) did not have a significantly higher or lower
557 importance for determining $\ln(\lambda)$ in comparison to less variable vital rates. This indicates that
558 vital rate buffering is not stabilizing $\ln(\lambda)$ after abiotic or demographic perturbation. The evidence
559 for spatial asynchrony and fine-scale source-sink dynamics was also not strong. Mantel tests did
560 not identify a significant relationship between the correlation of $\ln(\lambda)$ between subpopulations and
561 their spatial proximity, but did identify non-significant relationships between $\ln(\lambda)$ correlation and
562 proximity. However, this relationship was positive in Soapstone prairie subpopulations and negative
563 in FEWAFF subpopulations, which provides inconsistent support for these mechanisms.

564 It is somewhat surprising that negative density dependence is the only mechanism of small
565 population persistence that has significant support in *O. coloradensis* populations, since multiple
566 mechanisms have been identified in at least one other rare species (Dibner et al., 2019). It is possi-
567 ble that support for one or more of these persistence mechanisms could emerge if more information
568 about abiotic variation across space and time and data from more annual transitions was avail-
569 able for analysis. One potential explanation is that, while this species is a globally rare endemic
570 with isolated subpopulations, it often grows at high local density. This strategy, which Rabinowitz
571 describes as “locally abundant in a specific habitat but restricted geographically,” may allow *O.*
572 *coloradensis* to bypass the problems that small populations typically face, such as genetic and demo-
573 graphic bottlenecks that make them susceptible to stochastic environmental variation (Rabinowitz,
574 1981). It has also been shown that rare species are more likely than common species to benefit
575 from facilitative interspecific interactions (Calatayud et al., 2020). *O. coloradensis* may participate
576 in facilitative interactions with other species that increase its probability of persistence, although
577 determining this will require further, community-level analysis. Our results imply that not all rare

578 species can be treated equally. While demographic strategies that help maintain persistence may
579 be effective for some species, other species may employ different strategies. This further emphasizes
580 the importance of carefully considering the specific population and its community dynamics when
581 managing and conserving rare species.

582 Our analysis of the population dynamics of *Oenothera coloradensis* at two distinct locations
583 shows that this species has a life cycle that is strongly driven by introduction and persistence of
584 seeds into a seed bank. More broadly, we show that this rare endemic species shows signs of negative
585 density dependence. Populations of *O. coloradensis* may additionally be maintained via high local
586 abundances that allow them to escape the challenges of small population size that rare species
587 often face (Rabinowitz, 1981). These findings reinforce the importance of careful evaluation of the
588 unique population dynamics of rare species to inform successful conservation and management.

589 References

- 590 Abbott, R. E., Doak, D. F., & Peterson, M. L. (2017). Portfolio effects, climate change,
591 and the persistence of small populations: analyses on the rare plant *Saussurea weberi*.
592 *Ecology*, 98(4), 1071–1081. <https://doi.org/10.1002/ecy.1738>
- 593 Arnoldi, J. F., Loreau, M., & Haegeman, B. (2019). The inherent multidimensionality of
594 temporal variability: how common and rare species shape stability patterns. *Ecology*
595 *Letters*, 22(10), 1557–1567. <https://doi.org/10.1111/ele.13345>
- 596 Burgess, L. M., Hild, A. L., & Shaw, N. L. (2005). Capsule treatments to enhance seedling
597 emergence of *Gaura neomexicana* ssp. *coloradensis*. *Restoration Ecology*, 13(1), 8–14.
598 <https://doi.org/10.1111/j.1526-100X.2005.00002.x>
- 599 Burner, R. C., Drag, L., Stephan, J. G., Birkemoe, T., Wetherbee, R., Muller, J., Siito-
600 nen, J., Snäll, T., Skarpaas, O., Potterf, M., Doerfler, I., Gossner, M. M., Schall, P.,
601 Weisser, W. W., & Sverdrup-Thygeson, A. (2022). Functional structure of European
602 forest beetle communities is enhanced by rare species. *Biological Conservation*, 267.
603 <https://doi.org/10.1016/j.biocon.2022.109491>

- 604 Calatayud, J., Andivia, E., Escudero, A., Melián, C. J., Bernardo-Madrid, R., Stoffel, M.,
605 Aponte, C., Medina, N. G., Molina-Venegas, R., Arnan, X., Rosvall, M., Neuman,
606 M., Noriega, J. A., Alves-Martins, F., Draper, I., Luzuriaga, A., Ballesteros-Cánovas,
607 J. A., Morales-Molino, C., Ferrandis, P., ... Madrigal-González, J. (2020). Positive
608 associations among rare species and their persistence in ecological assemblages. *Nature
609 Ecology and Evolution*, 4(1), 40–45. <https://doi.org/10.1038/s41559-019-1053-5>
- 610 Caswell, H. (2001). *Matrix Population Models: Construction, Analysis, and Interpretation*
611 (2nd ed.). Sinauer Associates.
- 612 Dibner, R. R., Peterson, M. L., Louthan, A. M., & Doak, D. F. (2019). Multiple mechanisms
613 confer stability to isolated populations of a rare endemic plant. *Ecological Monographs*,
614 89(2), 1–16. <https://doi.org/10.1002/ecm.1360>
- 615 Drury, W. H. (1974). Rare species. *Biological Conservation*, 6(3), 162–169. [https://doi.org/10.1016/0006-3207\(74\)90061-5](https://doi.org/10.1016/0006-3207(74)90061-5)
- 616 Easterling, M. R., Ellner, S. P., & Dixon, P. M. (2000). Size-Specific Sensitivity: Applying
617 a New Structured Population Model. *Ecology*, 81(3), 694–708. [https://doi.org/10.1890/0012-9658\(2000\)081\[0694:SSSAAN\]2.0.CO;2](https://doi.org/10.1890/0012-9658(2000)081[0694:SSSAAN]2.0.CO;2)
- 618 Ellner, S. P., Childs, D. Z., & Rees, M. (2016). *Data-driven Modelling of Structured Popula-
619 tions*. Switzerland: Springer International Publishing. <https://doi.org/10.1007/978-3-319-28893-2>
- 620 Ellner, S. P., & Rees, M. (2006). Integral projection models for species with complex
621 demography. *American Naturalist*, 167(3), 410–428. <https://doi.org/10.1086/499438>
- 622 *Endangered and threatened wildlife and plants; removing Oenothera coloradensis (colorado
623 butterfly plant) from the federal list of endangered and threatened plants.* (2019). 50
624 C.F.R. pt. 17. (<https://www.federalregister.gov/documents/2019/11/05/2019-24124/endangered-and-threatened-wildlife-and-plants-removing-oenothera-coloradensis-colorado-butterfly>)
- 625 *Endangered and threatened wildlife and plants: Threatened status for the colorado but-
626 terfly plant (Gaura neomexicana ssp. coloradensis) from southeastern wyoming,
627 northcentral colorado, and extreme western nebraska.* (2000). 50 C.F.R. pt. 17.
628 (<https://www.federalregister.gov/documents/2000/10/18/00-26544/endangered-and->

- 634 threatened-wildlife-and-plants-threatened-status-for-the-colorado-butterfly-plant)
- 635 Enquist, B. J., Feng, X., Boyle, B., Maitner, B., Newman, E. A., Jørgensen, P. M.,
636 Roehrdanz, P. R., Thiers, B. M., Burger, J. R., Corlett, R. T., Couvreur, T. L.,
637 Dauby, G., Donoghue, J. C., Foden, W., Lovett, J. C., Marquet, P. A., Merow, C.,
638 Midgley, G., Morueta-Holme, N., ... McGill, B. J. (2019). The commonness of rarity:
639 Global and future distribution of rarity across land plants. *Science Advances*, 5(11),
640 1–14. <https://doi.org/10.1126/sciadv.aaz0414>
- 641 Fertig, W. (2000). *Status review of the Colorado butterfly plant (Gaura neomexicana ssp.*
642 *coloradensis*)
- (Tech. Rep.). Laramie, WY: Prepared for U.S. Fish and Wildlife Service and F. E. Warren Air Force Base by the Wyoming Natural Diversity Database (University of Wyoming).
- 643
- 644
- 645 Fieberg, J. R., Vitense, K., & Johnson, D. H. (2020). Resampling-based methods for
646 biologists. *PeerJ*, 2020(3). <https://doi.org/10.7717/peerj.9089>
- 647 Floyd, S. K., & Ranker, T. A. (1998). Analysis of a Transition Matrix Model for *Gaura*
648 *neomexicana* Ssp. *coloradensis* (Onagraceae) Reveals Spatial and Temporal Demo-
649 graphic Variability. *International Journal of Plant Sciences*, 159(5), 853–863.
- 650 Gaillard, J.-M., & Yoccoz, N. G. (2003). Temporal variation in survival of mammals: A case
651 of environmental canalization? *Ecology*, 84(12), 3294–3306.
- 652 Heidel, B., Tuthill, D., & Wallace, Z. (2021). *33-Year Population Trends of Colorado*
653 *Butterfly Plant (Oenothera Coloradensis; Onagraceae), a Short-Lived Riparian Species*
654 *on F. E. Warren Air Force Base, Laramie County, Wyoming* (Tech. Rep.). Laramie,
655 WY: Prepared for U.S. Fish and Wildlife Service and F. E. Warren Air Force Base by
656 the Wyoming Natural Diversity Database (University of Wyoming).
- 657 Hilde, C. H., Gamelon, M., Sæther, B. E., Gaillard, J. M., Yoccoz, N. G., & Pélabon, C.
658 (2020). The Demographic Buffering Hypothesis: Evidence and Challenges. *Trends in*
659 *Ecology and Evolution*, 35(6), 523–538. <https://doi.org/10.1016/j.tree.2020.02.004>
- 660 Kauffman, M. J., Pollock, J. F., & Walton, B. (2004). Spatial structure, dispersal, and
661 management of a recovering raptor population. *American Naturalist*, 164(5), 582–597.
662 <https://doi.org/10.1086/424763>
- 663 Levins, R., & Culver, D. (1971). Regional Coexistence of Species and Competition between

- 664 Rare Species. *Proceedings of the National Academy of Sciences*, 68(6), 1246–1248.
665 <https://doi.org/10.1073/pnas.68.6.1246>
- 666 Link, William A, Paul F Doherty, Fr. (2002). Scaling in sensitivity analysis. *Ecology*, 83(12),
667 3299–3305. <https://doi.org/10.2307/3072080>
- 668 Lyons, K. G., Brigham, C. A., Traut, B. H., & Schwartz, M. W. (2005). Rare species
669 and ecosystem functioning. *Conservation Biology*, 19(4), 1019–1024. <https://doi.org/>
670 [10.1111/j.1523-1739.2005.00106.x](https://doi.org/10.1111/j.1523-1739.2005.00106.x)
- 671 Magurran, A. E., & Henderson, P. A. (2011). Commonness and Rarity. In A. E. Magurran
672 & B. J. McGill (Eds.), *Biological diversity : frontiers in measurement and assessment*
673 (pp. 97–104). Oxford University Press.
- 674 May, R. M. (1973). Stability in Randomly Fluctuating Versus Deterministic Environments.
675 *The American Naturalist*, 107(957), 621–650.
- 676 McDonald, J. L., Franco, M., Townley, S., Ezard, T. H., Jelbert, K., & Hodgson, D. J.
677 (2017). Divergent demographic strategies of plants in variable environments. *Nature
678 Ecology and Evolution*, 1(2). <https://doi.org/10.1038/s41559-016-0029>
- 679 Merow, C., Dahlgren, J. P., Metcalf, C. J. E., Childs, D. Z., Evans, M. E., Jongejans, E.,
680 Record, S., Rees, M., Salguero-Gómez, R., & McMahon, S. M. (2014). Advancing
681 population ecology with integral projection models: A practical guide. *Methods in
682 Ecology and Evolution*, 5(2), 99–110. <https://doi.org/10.1111/2041-210X.12146>
- 683 Morris, W. F., & Doak, D. F. (2002). *Quantitative Conservation Biology: Theory and
684 Practice of Population Viability Analysis*. Sunderland, MA: Sinauer Associates.
- 685 Nei, M., Maruyama, T., & Chakraborty, R. (1975). The Bottleneck Effect and Genetic
686 Variability in Populations. *Evolution*, 29(1), 1–10.
- 687 Nguyen, V., Buckley, Y. M., Salguero-Gómez, R., & Wardle, G. M. (2019). Conse-
688 quences of neglecting cryptic life stages from demographic models. *Ecological Mod-
689 ellng*, 408(June). <https://doi.org/10.1016/j.ecolmodel.2019.108723>
- 690 Oksanen, J., Blanchet, F. G., Friendly, M., Kindt, R., Legendre, P., McGlinn, D., Minchin,
691 P. R., O'Hara, R. B., Simpson, G. L., Solymos, P., Stevens, M. H. H., Szoecs, E., &
692 Wagner, H. (2020). *vegan: Community Ecology Package*. R package version 2.5-7.
693 Retrieved from <https://cran.r-project.org/package=vegan>

- 694 Paniw, M., Quintana-Ascencio, P. F., Ojeda, F., & Salguero-Gómez, R. (2017). Accounting
695 for uncertainty in dormant life stages in stochastic demographic models. *Oikos*, 126(6),
696 900–909. <https://doi.org/10.1111/oik.03696>
- 697 Pfister, C. A. (1998). Patterns of variance in stage-structured populations : Evolutionary
698 predictions and ecological implications. *Proceedings of the National Academy of Sciences*, 95, 213–218.
- 700 PRISM Climate Group; Oregon State University. (2021). *PRISM Climate Group, Oregon*
701 *State University*. Retrieved from <https://prism.oregonstate.edu>
- 702 Pulliam, H. R. (1988). Sources, Sinks, and Population Regulation. *The American Naturalist*,
703 132(5), 652–661.
- 704 Rabinowitz, D. (1981). Seven forms of rarity. In H. Synge (Ed.), *The biological aspects of*
705 *rare plant conservation*. John Wiley & Sons, Ltd. <https://doi.org/10.2307/4110060>
- 706 Ramula, S., Rees, M., & Buckley, Y. M. (2009). Integral projection models perform better
707 for small demographic data sets than matrix population models: A case study of
708 two perennial herbs. *Journal of Applied Ecology*, 46(5), 1048–1053. <https://doi.org/10.1111/j.1365-2664.2009.01706.x>
- 710 Rees, M., Childs, D. Z., Metcalf, C. J. E., Rose, K. E., Sheppard, A. W., & Grubb, P. J.
711 (2006). Seed dormancy and delayed flowering in monocarpic plants: selective in-
712 teractions in a stochastic environment. *The American Naturalist*, 168(2), E53-E71.
713 <https://doi.org/10.1086/505762>
- 714 Rovere, J., & Fox, J. W. (2019). Persistently rare species experience stronger negative fre-
715 quency dependence than common species: A statistical attractor that is hard to avoid.
716 *Global Ecology and Biogeography*, 28(4), 508–520. <https://doi.org/10.1111/geb.12871>
- 717 Sgarbi, L. F., & Melo, A. S. (2018). You don't belong here: explaining the excess of rare
718 species in terms of habitat, space and time. *Oikos*, 127(4), 497–506. <https://doi.org/10.1111/oik.04855>
- 720 Spear, M. J., Walsh, J. R., Ricciardi, A., & Vander Zanden, M. J. (2021). The Invasion Ecol-
721 ogy of Sleeper Populations: Prevalence, Persistence, and Abrupt Shifts. *BioScience*,
722 71(4), 357–369. <https://doi.org/10.1093/biosci/biaa168>
- 723 Stanley, S. M. (1979). *Macroevolution: Pattern and Process*. W. H. Freeman.

- 724 Tuljapurkar, S. (1989). An Uncertain Life : Demography in Random Environments . *Theoretical
725 Population Biology*, 35, 227–294. [https://doi.org/10.1016/0040-5809\(89\)90001-4](https://doi.org/10.1016/0040-5809(89)90001-4)
- 726 Venables, W. N., & Ripley, B. D. (2002). *Modern Applied Statistics with S* (Fourth ed.).
727 New York: Springer. Retrieved from <https://www.stats.ox.ac.uk/pub/MASS4/>
- 728 Villegas, J., Doak, D. F., García, M. B., & Morris, W. F. (2015). Demographic compensation
729 among populations: What is it, how does it arise and what are its implications? *Ecology
730 Letters*, 18(11), 1139–1152. <https://doi.org/10.1111/ele.12505>
- 731 Vincent, H., Bornand, C. N., Kempel, A., & Fischer, M. (2020). Rare species perform worse
732 than widespread species under changed climate. *Biological Conservation*, 246, 108586.
733 <https://doi.org/10.1016/j.biocon.2020.108586>
- 734 Vitalis, R., Glémén, S., & Olivier, I. (2004). When genes go to sleep: The population genetic
735 consequences of seed dormancy and monocarpic perenniality. *American Naturalist*,
736 163(2), 295–311. <https://doi.org/10.1086/381041>
- 737 Wagner, W. L., Krakos, K. N., & Hoch, P. C. (2013). Taxonomic changes in oenothera
738 sections gaura and calylophus (onagraceae). *PhytoKeys*(28), 61–72. <https://doi.org/10.3897/phytokeys.28.6143>